

delocalization away from the silicon atom, and, hence, the silicon is shielded as compared to the phenylsilyl anions.

Conclusions

^{13}C NMR spectroscopic studies have shown that the delocalization of charge in phenylsilyl anions is significantly reduced as compared to the corresponding phenyl carbanions. Using the para-carbon shifts as a probe to the electron density in the phenyl rings, we found that the delocalization of charge was reduced by a factor of ~ 9 – 10 for Ph_3SiLi . This could be, to a large degree, due to the nonplanarity of the system, which would effectively reduce $p\pi$ – $p\pi$ overlap. For Ph_2MeSiLi and PhMe_2SiLi , the delocalization is only ~ 3 – 4 times less than that in the corresponding carbanion analogues. This is in contrast to the findings of A. G. Evans,¹⁷ who concluded from his UV studies that the conjugation between the silicon center and phenyl groups must be practically zero since replacement of phenyl by methyl has no effect on the λ_{max} of phenylsilyl anions. His conclusions are, however, probably correct in indicating that the phenyl groups are not conjugated with each other through silicon. As in the case of the study by Cox et al.,³ it is at this time still difficult to elucidate the exact mechanism for the electron delocalization ($d\pi$ or $p\pi$) in phenylsilyl anions although it is most likely $p\pi$ – $p\pi$.

The ^{29}Si NMR data are more difficult to interpret than the ^{13}C NMR data. Although $\Delta\delta_{29\text{Si}}$ of the chemical shifts for X_3SiM vs. X_3SiCl does follow a nearly linear plot, $\Delta\delta_{29\text{Si}}$ for X_3SiM vs. X_3SiH does not (where $\text{X} = \text{Me}$, Ph and $\text{M} = \text{Li}$ or K). The reason for this deviation could not be elucidated. For X_3SiM vs. X_3SiCl , the increase in $\Delta\delta_{29\text{Si}}$ indicates that, as a methyl group replaces a phenyl, an increase in shielding is observed. In respect to the ^{29}Si NMR shifts themselves, it is probable that they reflect primarily the amount of charge localized on the silicon atom, being most deshielded for PhMe_2SiLi and Ph_2MeSiLi where there is increased delocalization of charge per phenyl ring and most shielded for Me_3SiK where there is no significant delocalization into the methyl groups.

Experimental Section

Ph_3SiCl , Ph_3SiH , Ph_2MeSiCl , PhMe_2SiCl , and $\text{Me}_3\text{SiSiMe}_3$ were commercially available from Peninsular Research Chemicals, Inc.

Me_3SiCl was obtained from Aldrich Chemical Co. These silanes were not further purified. Lithium and $\text{KO-}t\text{-Bu}$ were obtained from Alfa-Ventron.

(Triphenylsilyl)lithium³³ was prepared by the treatment of triphenylchlorosilane with 4 equiv of lithium in dry THF, reacting under argon for four days. An aliquot of the solution was transferred by syringe to a dry argon flushed 10-mm NMR tube for spectroscopic study. (Diphenylsilyl)lithium and (methylphenylsilyl)lithium³³ were prepared similarly to (triphenylsilyl)lithium, except that in the case of (methylphenylsilyl)lithium, the reaction time was 1 day.

(Trimethylsilyl)potassium³⁴ was obtained by the treatment of hexamethylidisilane with an equimolar amount of $\text{KO-}t\text{-Bu}$ in HMPA at 0°C under argon. After the reaction was complete (~ 1 h at 0°C), the deep red solution was allowed to warm to room temperature and an aliquot was transferred via syringe and under argon to a dry 10-mm tube for NMR analysis.

Nuclear Magnetic Resonance Studies. ^{13}C NMR studies were carried out by using a Varian FT-80 NMR spectrometer equipped with a broad-band decoupler, variable-temperature probe, and 32K memory capacity computer. Chemical shifts were measured from Me_4Si (internal) in the case of neutral compounds and from solvent THF in the case of the silyl anions (THF, $\alpha = 26.2$, $\beta = 78.0$).

^{29}Si NMR studies were carried out on a Varian FT-80 NMR spectrometer operating at 15.801 MHz by using a variable-temperature probe equipped with a broad-band decoupler. Proton heteronuclear decoupling was performed during these experiments. In the case of neutral silanes, internal Me_4Si was used as reference. For the silicon anions, the spectrometer was zeroed by using a $\text{Me}_4\text{Si}/\text{THF}$ sample and the ^{29}Si NMR of the anion solution was recorded immediately afterwards. Signals deshielded from Me_4Si were considered positive while those shielded were considered negative. Typically, a pulse width of $5\ \mu\text{s}$, pulse delay of 10–20 s, and sweep width of 8000 Hz were used. The decoupler was turned on during acquisition and off during the pulse delay in order to suppress the negative NOE of silicon-29.

Acknowledgment. Support of our work by the National Institutes of Health and the National Science Foundation is gratefully acknowledged.

(33) George, M. V.; Peterson, P. J.; Gilman, H. *J. Am. Chem. Soc.* **1960**, *82*, 403. Gilman, H.; Peterson, D. J.; Wittenberg, P. *Chem. Ind.* **1958**, 1479.

(34) Saburai, H.; Okada, A.; Kira, M.; Yonegawa, K. *Tetrahedron Lett.* **1971**, 1511.

An Electronic Spectroscopic Study of Iron Coordination in Hemerythrin

Joann Sanders Loehr,^{*1a} Thomas M. Loehr,^{1b} A. Grant Mauk,^{1c} and Harry B. Gray

Contribution No. 6217 from the Arthur Amos Noyes Laboratory of Chemical Physics, California Institute of Technology, Pasadena, California, 91125. Received April 28, 1980

Abstract: Electronic spectroscopy in the near-IR region reveals the presence of Fe(III) ligand field bands at 990 nm in oxyhemerythrin, at 970 and 1050 nm in methemerythrin(N_3), and at 935 and 1040 nm in methemerythrin(OH). These bands are assigned as the ${}^6\text{A}_1 \rightarrow {}^4\text{T}_1({}^4\text{G})$ transitions of octahedrally coordinated high-spin Fe(III) centers. The resolution of two components in the spectra of the methemerythrins is attributed to inequivalent ligation of the two active-site Fe(III) ions by two and three histidines, respectively. The spectrum of deoxyhemerythrin is also characteristic of octahedral iron coordination, with bands at 855 and 1110 nm being associated with a split ${}^5\text{T}_2 \rightarrow {}^5\text{E}$ ligand field system of high-spin Fe(II). The near-IR spectrum of the half-reduced hemerythrin(N_3) intermediate exhibits a band at 1190 nm ($\epsilon = 16\ \text{M}^{-1}\ \text{cm}^{-1}$ per Fe atom); it is proposed that this band arises mainly from Fe(II) ligand field excitation and that the intensity enhancement comes from partial electron delocalization in the $[\text{Fe(II)}^*, \text{Fe(III)}]$ excited state.

Introduction

Hemerythrin is an invertebrate respiratory protein which contains two nonheme iron atoms at each oxygen-binding site.^{2,3}

In both oxyhemerythrin and methemerythrin, the pair of iron atoms have been identified as antiferromagnetically coupled, high-spin Fe(III) by Mössbauer spectroscopy and magnetic susceptibility measurements.⁴ The ligand field (LF) bands in

(1) (a) Department of Chemistry, Portland State University, Portland, Oregon 97207. (b) Department of Chemistry and Biochemical Sciences, Oregon Graduate Center, Beaverton, Oregon 97006. (c) Department of Biochemistry, The University of British Columbia, Vancouver, B.C., Canada, V6T 1W5.

(2) Kurtz, D. M., Jr.; Shriver, D. F.; Klotz, I. M. *Coord. Chem. Rev.* **1977**, *24*, 145–178.

(3) Stenkamp, R. E.; Jensen, L. H. *Adv. Inorg. Biochem.* **1979**, *1*, 219–233.

Table I. Assignments of Ligand Field Bands in High-Spin, Octahedral Fe(III) Complexes and Hemerythrins^a

	⁶ A ₁ → ⁴ T ₂ (⁴ D)	⁶ A ₁ → [⁴ A ₁ , ⁴ E](⁴ G)	⁶ A ₁ → ⁴ T ₂ (⁴ G)	⁶ A ₁ → ⁴ T ₁ (⁴ G)
NaMgFe(oxalate) ₃ ·9H ₂ O ^b	445 [1.2]	450 [2.0]	670 [1.1]	950 [1.0]
(NH ₄) ₃ Fe(malonate) ₃ ^c	390	435 [2.4]	635 [0.9]	900 [0.7]
[(DPM) ₂ Fe(OCH ₃) ₂] ₂ ^d			710 [2.0]	935 [1.0]
EnH ₂ [(FeHEDTA) ₂ O]·6H ₂ O ^e	405 [120]	475 [25]	545 [40]	895 [2.6]
MetHr(N ₃)			680 [92]	1010 [5.1] { 970 [2.5] ^f 1050 [2.9] ^f
MetHr(OH)		480 [302]	610 [73]	990 [4.0] { 935 [2.1] ^f 1040 [2.6] ^f
OxyHr			750 [103]	990 [5.0] ^f
semi-metHr(N ₃)			730 [~40]	910 [~10] ^f
semi-metHr(OH)		490 [~180]	670 [~40]	995 [~4] ^f

^a λ (in nm) at maximum absorbance for resolved bands. [ε_{max} in M⁻¹ cm⁻¹ per Fe atom] calculated from absorption envelope. Protein concentration based on ε₂₈₀ = 17 700 M⁻¹ cm⁻¹ per Fe atom.¹⁰ Values below 900 nm accurate to ±5 nm for λ and ±5% for ε. Values above 900 nm accurate to ±20 nm for λ and ±20% for ε. Semi-metHr values for ε are ±30% due to difficulty of obtaining samples which are free of both metHr and deoxyHr. ^b Holt, S.; Dingle, R. *Acta Chem. Scand.* 1968, 22, 1091-1096. ^c Hatfield, W. E. *Inorg. Chem.* 1964, 3, 605-606. ^d Wu, C. S.; Rossman, G. R.; Gray, H. B.; Hammond, G. S.; Schugar, H. J. *Inorg. Chem.* 1972, 11, 990-994. DPM = dipivaloylmethane. ^e Schugar, H. J.; Rossman, G. R.; Barraclough, C. G.; Gray, H. B. *J. Am. Chem. Soc.* 1972, 94, 2683-2690. HEDTA = *N*-hydroxyethyl-ethylenediaminetriacetate. ^f ε_{max} calculated from intensity of resolved band.

the electronic spectra of oxy- and methemerythrin have considerably greater intensities than the corresponding bands of monomeric, octahedral, high-spin Fe(III) complexes.³ The observed intensity enhancement could be a consequence either of the spin-spin interaction between the two iron atoms or a distortion of the octahedral ligand field about the iron atoms, or both. Although X-ray crystallographic structures of methemerythrin and metmyohemerythrin indicate that the two iron atoms are in octahedral coordination sites,³ the resolution is not adequate to determine the degree of regularity of the active-site structures. Thus, additional spectroscopic investigations could be helpful in determining the coordination geometry of iron in hemerythrin.

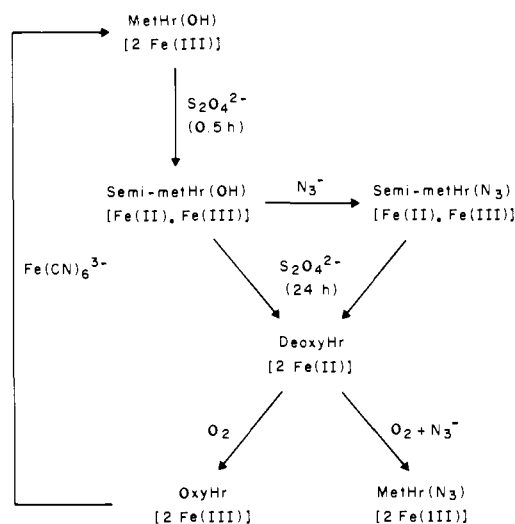
All octahedral Fe(II) and Fe(III) complexes exhibit characteristic LF absorption bands in the near-IR region of the spectrum. However, a previous study⁶ of the electronic absorption spectra of oxyhemerythrin and metaquoemerythrin failed to resolve any of these characteristic bands. The present work was undertaken to examine thoroughly the near-IR spectra of several hemerythrin derivatives, including deoxyhemerythrin and the newly described intermediate, semi-methemerythrin.⁷ Low-energy bands attributable to LF transitions in octahedrally coordinated iron were observed for all of the hemerythrin (Hr) species diagrammed in Scheme I.

Experimental Section

Hemerythrin. Hr was obtained from the sipunculid, *Phascolopsis gouldii*, as described previously.⁸ Crystallized oxyHr was converted to metHr(OH) by treatment with a twofold excess of K₃Fe(CN)₆ in 0.05 M Tris-SO₄ (pH 9.0).⁹ After dialysis to remove excess K₃Fe(CN)₆, the protein was concentrated eightfold by ultrafiltration through an XM-50 Amicon membrane and then mixed with an eightfold excess of 0.05 M Tris-SO₄ in 99.8% D₂O (pD 9.4). The ultrafiltration and dilution steps were repeated twice, followed by a final ultrafiltration to give a solution ~0.005 M in hemerythrin monomer (~0.01 M in Fe). The final ultrafiltrate was used as a buffer blank. All solutions were passed through sterile 0.45 μm Millipore filters prior to any spectroscopic measurements. Deuterated buffer was prepared by dissolving Tris base in 10 mL of D₂O (BioRad, 99.8%), adjusting the pD with a few drops of concentrated H₂SO₄, lyophilizing to dryness, and redissolving in 100 mL of D₂O.

MetHr(OH) was reduced to semi-methemerythrin(OH), abbreviated as [semi-met(OH)],¹⁰ in an N₂-equilibrated drybox by using a cold plate

Scheme I



to maintain all solutions at ~4 °C. Stopped vials containing metHr(OH), deuterated buffer (±azide), and solid Na₂S₂O₄ were degassed with Ar prior to placement into the drybox. Freshly prepared 0.2 M Na₂S₂O₄ was added dropwise with stirring to give a twofold molar excess of Na₂S₂O₄ to Fe in metHr(OH), and the resulting solution was filtered into a gas-tight cuvette. [Semi-met(N₃)] was prepared by allowing the dithionite reduction to proceed for 20 min at room temperature to get complete conversion of metHr(OH) to [semi-met(OH)] before the dropwise addition of 0.5 M NaN₃ (final concentration 0.02 M).

Spectra of deoxyHr were recorded after the dithionite reduction was allowed to proceed for 24 h at room temperature. Spectra of oxyHr were recorded 1 h after addition of excess O₂ to deoxyHr. To obtain metHr(N₃), we equilibrated deoxyHr plus azide with excess O₂ for 2 weeks at 4 °C. Hemerythrin concentrations were determined from the absorbance at 280 nm of diluted solutions by using ε₂₈₀ = 17 700 M⁻¹ cm⁻¹ per Fe atom.¹¹

Fe(EDTA)²⁻. Equal volumes of Ar-equilibrated solutions of 0.2 M Fe(NH₄)₂(SO₄)₂·6H₂O in 99.8% D₂O and 0.24 M Na₂H₂EDTA·2H₂O in 99.8% D₂O were mixed anaerobically with some loss of solvent to give a final concentration of 0.14 M Fe (as judged by atomic absorption spectroscopy) and pD 5.4.

Spectral Measurements. Visible and near-IR spectra were obtained on a Cary 17 spectrophotometer, using hemerythrin samples in 0.05 M Tris-SO₄, > 95% D₂O (pD 9.4). Solutions were placed in a 1.0-cm path length cell in a jacketed cell holder connected to a refrigerated bath. Ultraviolet spectra were recorded on a Cary 118 spectrophotometer. Visible and near-IR spectra were replotted on an energy scale after the spectrum of the deuterated buffer was subtracted. The resulting spectra

(4) Loehr, J. S.; Loehr, T. M. *Adv. Inorg. Biochem.* 1979, 1, 235-252.

(5) Gray, H. B. *Adv. Inorg. Biochem.* 1980, 2, 1-25.

(6) Dawson, J. W.; Gray, H. B.; Hoening, H. E.; Rossman, G. R.; Schredder, J. M.; Wang, R.-H. *Biochemistry* 1972, 11, 461-465.

(7) Harrington, P. C.; DeWaal, D. J. A.; Wilkins, R. G. *Arch. Biochem. Biophys.* 1978, 191, 444-451.

(8) Klotz, I. M.; Klotz, T. A.; Fiess, H. A. *Arch. Biochem. Biophys.* 1957, 68, 284-299.

(9) Keresztes-Nagy, S.; Klotz, I. M. *Biochemistry* 1965, 4, 919-931.

(10) This species is equivalent to [semi-met]_R described by: Babcock, L. M.; Bradič, Z.; Harrington, P. C.; Wilkins, R. G.; Yoneda, G. S. *J. Am. Chem. Soc.* 1980, 102, 2849-2850.

(11) Dunn, J. B. R.; Addison, A. W.; Bruce, R. E.; Loehr, J. S.; Loehr, T. M. *Biochemistry* 1977, 16, 1743-1749.

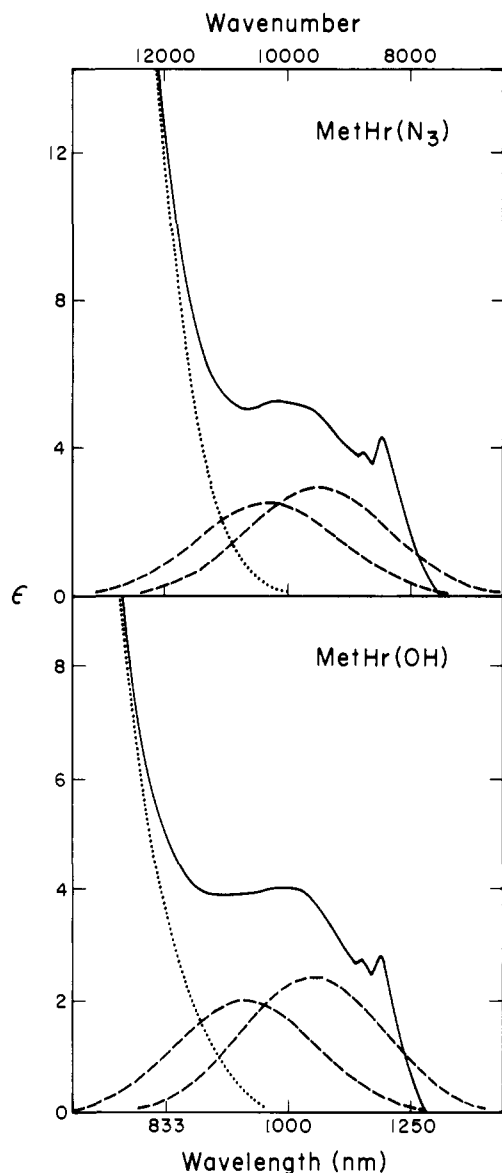


Figure 1. Near-IR spectra of methemerythrin(N₃) and methemerythrin(OH). Dashed lines represent Gaussian components. Dotted line represents remaining intensity after subtraction of Gaussian components.

were resolved with the smallest number of Gaussian curves, each with a width at half-height of $2700 \pm 100 \text{ cm}^{-1}$ unless otherwise noted.

Results and Discussion

Methemerythrin. The near-IR spectra of metHr(N₃) and metHr(OH) are shown in Figure 1. In both cases there is a distinct shoulder at $\sim 1000 \text{ nm}$ on the previously reported visible absorption band at 680 and 610 nm, respectively^{6,9} (Table I). The superior resolution in the near-IR region in the present study is due to the careful handling of concentrated solutions to prevent denaturation, particularly during dilution for ultrafiltration, and to the use of Millipore filtration to produce spectrally clear solutions. The fine structure at $\sim 1200 \text{ nm}$ is ascribed to vibrational modes characteristic of proteinaceous material. The steep drop in intensity at $\sim 1250 \text{ nm}$ is an artifact of the subtraction of the deuterated buffer spectrum. Deuterated buffer solutions show greater absorptivity in this spectral region than the concentrated hemerythrin solutions, despite the fact that the protein and reference solutions are matched in H₂O content and have equal intensity in the $\sim 1400\text{-nm}$ residual H₂O band.

Octahedral, high-spin Fe(III) complexes (⁶A₁ ground state) generally exhibit a series of four LF transitions in the visible and near-IR spectral region which are assigned as ⁶A₁ → ⁴T₂(⁴D), → [⁴A₁, ⁴E](⁴G), → ⁴T₂(⁴G), and → ⁴T₁(⁴G) in order of decreasing

energy.¹² Table I lists these four lowest LF transitions for a number of Fe(III) complexes. The low intensity shoulder ($\sim 1000 \text{ nm}$) in the spectra of metHr(N₃) and metHr(OH) is positioned correctly to be the ⁶A₁ → ⁴T₁(⁴G) transition, thereby providing convincing evidence for octahedrally coordinated Fe(III) in methemerythrin. The near-IR spectral information is crucial to this assignment since the higher energy LF bands in methemerythrin are obscured by intense ligand-metal charge-transfer absorption.¹³

The LF transition at $\sim 1000 \text{ nm}$ in metHr(N₃) and metHr(OH) has an enhanced intensity ($\epsilon \approx 4.5$) in comparison with the monomeric iron(III)-oxalate and iron(III)-malonate complexes listed in Table I. This is consistent with the previously observed enhancements¹³ of the metHr(N₃) LF band at 680 nm and the metHr(OH) LF bands at 610 and 480 nm when being compared with monomeric iron complexes. The pattern of intensity enhancement in the LF transitions of metHr(N₃) and metHr(OH) is most closely matched by μ -oxo-bridged ferric dimers such as (FeHEDTA)₂O²⁻. Similar conclusions regarding the usefulness of μ -oxo-bridged species as models for hemerythrin have been drawn from magnetic susceptibility measurements.⁶ X-ray crystallographic studies have led to proposals of two different structures for the active site of methemerythrin: one in which the irons are bridged by a μ -oxo group¹⁴ and one in which the irons are bridged by two protein carboxylate residues.³ The latter structure is difficult to evaluate due to the lack of suitable model carboxylate-bridged iron complexes. The closest available model compounds are the dihydroxo- and dialkoxo-bridged ferric dimers such as [(DPM)₂Fe(OCH₃)₂]₂. But, as seen from the results in Table I and from magnetic susceptibility studies,⁶ these (OR)₂-bridged compounds are not good models for the magnetic and spectroscopic properties of methemerythrin.

The band at $\sim 1000 \text{ nm}$ in the spectra of metHr(N₃) and metHr(OH) can be resolved into two contributing components (Figure 1). According to the X-ray crystallographic results for metHr³ and metmyoHr,¹⁴ one of the iron atoms is ligated to three N's (histidine) and two-three O's (carboxylate or water), whereas the other iron atom is ligated to two N's (histidine) and three O's (tyrosinate, carboxylate, or water) not counting the exogenous ligand site. Our results suggest that in metHr(OH) the ⁶A₁ → ⁴T₁(⁴G) transitions of the two Fe(III) centers are separated by 1100 cm^{-1} , which is consistent with the X-ray structural models. The lower energy transition (1040 nm) presumably is associated with the Fe(III) that is situated in the stronger LF environment (three N's). The higher energy component (935 nm) in metHr(OH) exhibits a larger shift upon conversion to metHr(N₃) than the lower energy feature. This could indicate preferential binding of azide to the two N-three O iron atom, as has been suggested from crystallographic¹⁴ and polarized single-crystal spectroscopic studies.¹⁵ Thus electronic spectroscopy, unlike Mössbauer spectroscopy,¹³ has quite clearly indicated the inequivalent ligation of the iron atoms in methemerythrin.

Oxyhemerythrin. The near-IR spectrum of oxyHr also contains evidence for a low-energy LF transition close to 1000 nm (Figure 2). Despite the high intensity and low energy of the adjacent LF band at 750 nm,¹³ an additional Gaussian component at 990 nm can be resolved from the absorption envelope in Figure 2. The peaks at 750 and 990 nm appear to correspond to the ⁶A₁ → ⁴T₂(⁴G) and ⁶A₁ → ⁴T₁(⁴G) LF bands observed for metHr (Table I) and support the conclusion from other spectroscopic and magnetic susceptibility studies⁴ that both oxyHr and metHr contain octahedrally coordinated and antiferromagnetically coupled high-spin Fe(III) ions. Although the resolution is too poor to observe contributions from two different iron atoms in the 1000-nm region, polarized single-crystal spectra of oxyHr do indicate a splitting in the 750-nm region.¹⁶ Furthermore,

(12) Hush, N. S.; Hobbs, R. J. M. *Prog. Inorg. Chem.* **1968**, *10*, 259-359.

(13) Garbett, K.; Darnall, D. W.; Klotz, I. M.; Williams, R. J. P. *Arch. Biochem. Biophys.* **1969**, *135*, 419-434.

(14) Hendrickson, W. A. *Nat. Rev.* **1978**, *31*, 1-20.

(15) Gay, R. R.; Solomon, E. I. *J. Am. Chem. Soc.* **1978**, *100*, 1972-1973.

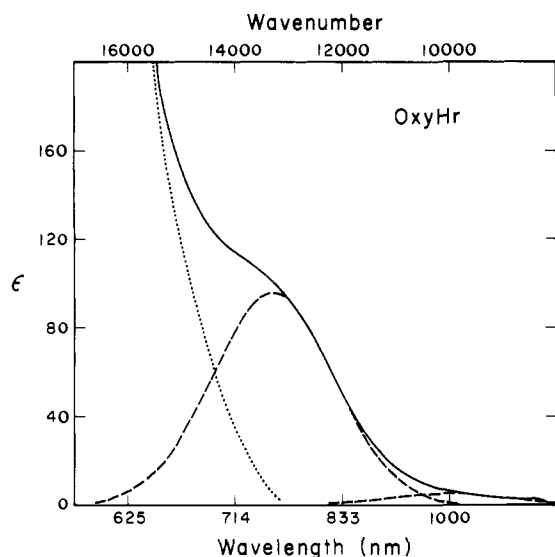


Figure 2. Visible and near-IR spectrum of oxyhemerythrin.

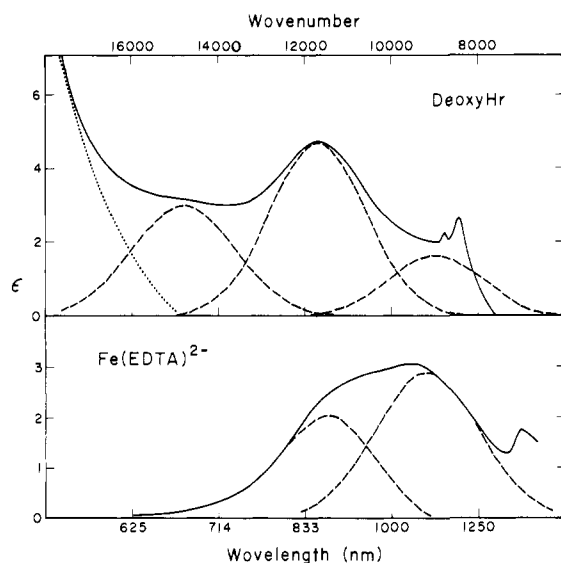


Figure 3. Visible and near-IR spectra of deoxyhemerythrin and Fe(EDTA)²⁻.

Mössbauer spectroscopic studies have shown inequivalent iron atoms in oxyhemerythrin.¹³ Thus we have little doubt that further electronic spectroscopic studies will reveal slightly different energies for the ${}^6A_1 \rightarrow {}^4T_1({}^4G)$ transitions in the two Fe(III) centers in oxyhemerythrin.

Deoxyhemerythrin. Treatment of metHr(OH) with excess dithionite for 24 h at room temperature causes nearly complete reduction to deoxyHr. The absorption spectrum (Figure 3) shows that the remaining intensity at 670 nm is less than 10% of the absorbance normally observed for [semi-met(OH)] (Table I and see below) with even less contribution from any residual metHr(OH) at 610 nm. The rest of the absorption envelope in the near-IR region can be resolved into a more intense band at 855 nm and a smaller band at 1110 nm. The appearance of two bands in the near-IR region is characteristic of octahedral, high-spin ferrous complexes (Table II), with Fe(EDTA)²⁻ providing a particularly good match for the observed frequencies in deoxyHr (Figure 3). A high-spin d^6 system in an octahedral field is expected to exhibit a ${}^5T_2 \rightarrow {}^5E$ LF transition; the observed splitting (Table II) can be attributed to the fact that the symmetry

Table II. Ligand Field Bands (${}^5T_2 \rightarrow {}^5E$) in High-Spin, Octahedral Fe(II) Complexes and Deoxyhemerythrin^a

Fe(H ₂ O) ₆ ²⁺ ^b	960 [1.7]	1205 [1.3]
Fe(py) ₆ Cl ₂ ^c	970 (0.37)	1170 (0.31)
Fe(EDTA) ²⁻	870 [2.5]	1085 [3.0]
deoxyHr	855 [4.8]	1110 [2.1]

^a λ and ϵ_{\max} as in Table I. ^b Cotton, F. A.; Meyers, M. D. J. *Am. Chem. Soc.* **1960**, *82*, 5023-5026. ^c Goodgame, D. M. L.; Goodgame, M.; Hitchman, M. A.; Weeks, M. J. *Inorg. Chem.* **1966**, *5*, 635-638. The absorbance values in parentheses are from reflectance spectra. py = pyridine.

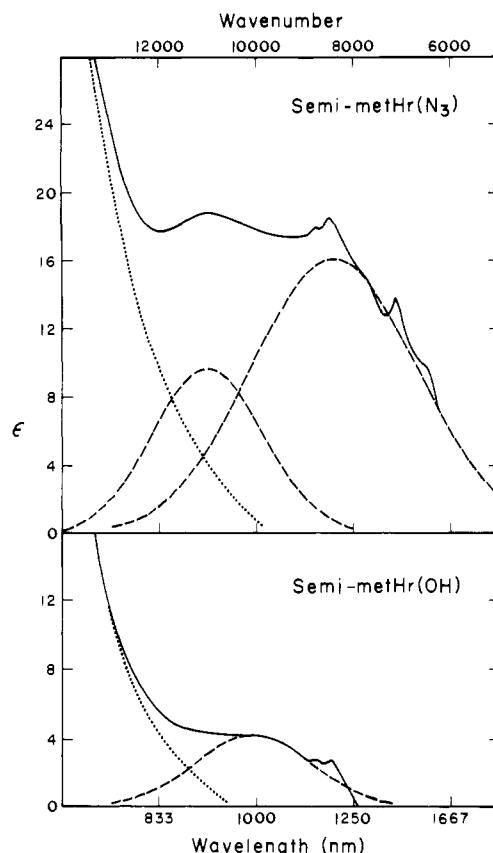


Figure 4. Near-IR spectra of semi-metHr(N₃) and semi-metHr(OH) recorded at 0.7 and 0.4 h, respectively, after addition of dithionite. Samples at ~ 4 °C. Resolved peak at 1190 nm has a band width of 4000 cm^{-1} .

at each Fe(II) center is slightly lower than octahedral. Additional splitting due to inequivalent iron atoms would be less significant in deoxyHr than in metHr as a result of a lower ligand field in ferrous complexes.

The intensities of the Fe(II) bands in deoxyHr are similar to those of other Fe(II) complexes (Table II), indicating that the magnetic interaction between the two iron atoms is substantially smaller in deoxyHr than in the more oxidized forms of hemerythrin. Magnetic susceptibility measurements have led to similar conclusions.⁴

Semi-metHr. The semi-metHr intermediate which is formed during the dithionite reduction of metHr to deoxyHr is difficult to prepare quantitatively but can be stabilized by holding the temperature near 4 °C. According to Harrington et al.,⁷ the reduction of metHr(OH) to [semi-met(OH)] has a rate constant of $\sim 10^5 \text{ M}^{-1} \text{ s}^{-1}$, whereas the reduction of [semi-met(OH)] to deoxyHr has a rate constant of $\sim 5 \times 10^{-4} \text{ s}^{-1}$ at 25 °C. Under our conditions of high protein concentration in D₂O, the rate of reduction of [semi-met(OH)] to deoxyHr was ~ 3 times slower at 25 °C and ~ 20 times slower at 4 °C than the value reported by Harrington et al. for less concentrated solutions in H₂O.

[Semi-met(N₃)] was prepared from [semi-met(OH)] which had been held at room temperature for 20 min prior to the addition

(16) Eickman, N. C.; Gay, R. R.; Penfield, K. W.; Himmelwright, R. S.; Loomis, L. D.; Solomon, E. I. "Invertebrate Oxygen-Binding Proteins: Structure, Active Site and Function"; Lamy, J., Lamy, J., Eds; Marcel Dekker: New York, 1980, in press.

of azide and cooling of the mixture to 4 °C. From the known rate of reduction, the amount of deoxyHr was close to 10% in the 0.7-h sample of [semi-met(N₃)] used for spectral measurement (Figure 4). The sample for the 0.4-h spectrum of [semi-met(OH)] (Figure 4) was maintained at ~4 °C from the time of addition of dithionite and, thus, contained only 3% deoxyHr. The amount of unreduced metHr(N₃) and metHr(OH) as judged by remaining intensity at 680 and 610 nm, respectively, was 2% for the 0.7-h sample of [semi-met(N₃)] and 5% for the 0.4-h sample of [semi-met(OH)].

The half-reduced forms are characterized by shifts in the Fe(III) LF bands from 680 nm in metHr(N₃) to 730 nm in [semi-met(N₃)] and from 480 and 610 nm in metHr(OH) to 490 and 670 nm, respectively, in [semi-met(OH)] (Table I). The near-IR spectrum of [semi-met(OH)] probably contains an Fe(II) component at ~850 nm in addition to the distinct Fe(III) component at 995 nm (Figure 4). In the [semi-met(N₃)] spectrum near-IR peaks are clearly observed at 910 and 1190 nm (Figure 4). The presence of the latter two spectral features is entirely consistent with formulation of the binuclear iron unit in [semi-met(N₃)] as a class II¹⁷ mixed-valence system. The 910-nm band very likely includes contributions both from Fe(II) and Fe(III) transitions. The broad 1190-nm absorption ($\Delta\bar{\nu}_{1/2} = 4000 \text{ cm}^{-1}$; $\epsilon = 16 \text{ M}^{-1} \text{ cm}^{-1}$) is probably derived from Fe(II) LF excitation, with a degree of electron delocalization (intervalence character) in the [Fe(II)*, Fe(III)] excited state as a possible explanation for the enhanced intensity.¹⁸

(17) Robin, M. B.; Day, P. *Adv. Inorg. Chem. Radiochem.* **1967**, *10*, 247-405.

(18) Smith, G. *Phys. Chem. Miner.* **1978**, *3*, 375-383.

In addition to the 1190 nm [Fe(II)*,Fe(III)] band observed for [semi-met(N₃)], both [semi-met(N₃)] and [semi-met(OH)] exhibit low-temperature EPR signals typical of an $S = 1/2$ [Fe(II),Fe(III)] system,¹⁹ presumably arising from the spin-spin interaction of $S = 2$ Fe(II) and $S = 5/2$ Fe(III) ions. However, an [Fe(II)*,Fe(III)] band was not detected in the near-IR spectrum of [semi-met(OH)]. Clearly, N₃⁻ plays an important role in enhancing the [Fe(II)*,Fe(III)] band intensity in [semi-met(N₃)]; the structural implications of this finding, however, remain to be elucidated.

Conclusions

The electronic spectra of methemerythrin, oxyhemerythrin, and semi-methemerythrin have ligand field bands characteristic of octahedral Fe(III) complexes while the electronic spectrum of deoxyhemerythrin is typical of octahedral Fe(II) species. The two iron atoms in hemerythrin can, therefore, by unequivocally assigned to octahedral symmetry in all three oxidation states of the protein. Among the best models for the iron sites in hemerythrin are the iron-EDTA complexes, which share the property of having similar numbers of N and O ligands.

Acknowledgment. We are grateful to Dr. Patricia C. Harrington and Dr. Vincent Miskowski for many helpful discussions. This research was supported by grants from the National Science Foundation (Grant CHE 77-11389) and the National Institutes of Health (Grant GM 18865).

(19) Muhoberac, B. B.; Wharton, D. C.; Babcock, L. M., Department of Biochemistry, University of Texas Health Science Center, and Harrington, P. C.; Wilkins, R. G., Department of Chemistry, New Mexico State University, 1980, personal communication.

Synthesis, Structures, Stabilities, and Reactions of Cationic Olefin Complexes of Palladium(II) Containing the η^5 -Cyclopentadienyl Ligand¹

Hideo Kurosawa,* Tetsuro Majima, and Naonori Asada

Contribution from the Department of Petroleum Chemistry, Osaka University, Suita, Osaka 565, Japan. Received January 2, 1980

Abstract: Syntheses of various cationic olefin complexes of palladium(II), [Pd(η^5 -C₅H₅)(PR₃)(olefin)]X (R = Ph, Et, *n*-Bu; X = ClO₄, BF₄), **4**, a class of compounds much more stable than hitherto known, are reported. **4** exhibited ¹H and ¹³C NMR spectral aspects remarkably well-defined for an olefin-palladium complex, providing means of studying configurations and relative stabilities in some detail. In **4** containing substituted styrenes, ¹³C NMR shifts of the olefin carbons correlate with the Hammett σ^+ parameters, while stabilities of the complexes correlate better with σ than σ^+ . A possible significance of ion pair formation in determining stability trends has been suggested. Olefin ligands rotate more rapidly about the palladium-olefin axis than the platinum-olefin axis. This result, as well as a different substituent dependency of the stability in series of substituted styrene complexes of palladium(II) and platinum(II), is explained in terms of less effective π back-bonding from palladium to olefin than from platinum. The ethylene complex of type **4** reacts with some nucleophiles to give alkyl complexes, Pd(η^5 -C₅H₅)(PPh₃)(CH₂CH₂Y) [Y = CH(COMe)₂, **9**, OR **10**], a class of compounds again remarkably stable for a substituted ethylpalladium(II) complex. ¹H NMR spectra of **9** and **10** prepared from the *cis*- and *trans*-ethylene-*d*₂ complexes indicated the *trans* addition of Pd and Y to ethylene. **9** and **10** undergo thermolysis via β -hydrogen elimination which is suggested to proceed through predissociation of PPh₃. The role of the η^5 -C₅H₅ ligand in raising stabilities of olefin and alkyl complexes of palladium(II) has been discussed in the light of the data.

A wide variety of synthetic reactions mediated by palladium utilize olefin-palladium(II) complexes as starting materials or as crucial intermediates.² Nevertheless, in contrast to extensive olefin-platinum(II) chemistry, a rather limited number of studies have been reported on olefin complexes of palladium(II) with a

particular emphasis on the nature of the metal-olefin bond or reactivities bearing on elementary steps involved in the synthetic reactions. This is clearly attributed, in part, to rather a labile character of the bond between palladium(II) and olefins, especially simple monoolefins whose complexes might lack such extra stabilization as is found in chelate complexes of diolefins or olefins containing donor atoms.³ Studies using simple monoolefins appear

(1) Part of this work has been presented at the ACS-CSJ Chemical Congress, April, 1979, Honolulu, Hawaii, Inor. 227.

(2) Maitlis, P. M. "The Organic Chemistry of Palladium"; Academic Press: New York, 1971; Vol. 2.

(3) Reference 2, Vol 1, pp 106.